Materials Transactions, Vol. 42, No. 1 (2001) pp. 2 to 13
Special Issue on Recent Progress in Understanding of Materials Fracture

OVERVIEW

Dislocation Modelling of Fatigue Cracks: An Overview

Franz Oswald Riemelmoser[1], Peter Gumbsch[1] and Reinhard Pippan[2]

[1] *Max-Planck-Institut für Metallforschung, Seestr. 92, D-70174 Stuttgart, Germany*
[2] *Erich-Schmid-Institute of Materials Science, Jahnstr. 12, A-8700 Leoben, Austria*

The intrinsic threshold behavior of fatigue cracks and the disappearance of any cyclic plastic deformation below a threshold value can be understood by taking into account the discreteness of plasticity with recourse to discrete dislocation models. The aim of this paper is to document the progress in the discrete dislocation modelling within the past twenty years and the resulting increase in the understanding of fatigue cracks. The problems addressed are (1) the nature of the intrinsic fatigue threshold, (2) the influence of microstructure and/or of the mean stress level on the crack tip deformation and (3) the physical reason for the minimum striation spacing at small stress intensity ranges. A particular purpose of this paper is to compare the different dislocation models proposed in the literature in order to differentiate aspects of fatigue crack growth that do and do not depend on modelling and on microstructural details.

(Received July 19, 2000; Accepted October 20, 2000)

Keywords: *fatigue crack, threshold of stress intensity, dislocation modelling, microstructure*

1. Introduction

The established picture of fatigue crack propagation rests on the pioneering work of Paris,[1)] Elber,[2)] Ritchie and Suresh[3)] and many others that cannot be named here separately. Paris recognized that fatigue crack propagation is controlled by the applied stress intensity range ΔK. This opened the way for the analysis of fatigue crack growth in terms of fracture mechanics, which had just reached the maturity to be applied to cyclic plastic crack problems.[4)] The following concentration on local processes during fatigue crack propagation let Elber realize that only a certain portion of the applied loading amplitude is actually transferred to the crack tip. He reasoned that the crack flanks make contact during the unloading sequence such that the crack tip is partly shielded from the remote cyclic loading which becomes less effective for crack propagation. Ritchie and Suresh investigated and categorized the physical mechanisms leading to the crack tip shielding. They introduced the terms *extrinsic* fatigue crack resistance and *intrinsic* fatigue resistance for the crack flank contact and for the material specific resistance, respectively. Paris' ΔK dependence of fatigue crack propagation is the result of the dominance of intrinsic processes while the commonly observed mean load dependence (or equivalently the $K_{\max}$ dependence) for near threshold crack propagation is attributed to extrinsic phenomena.

Extrinsic effects and their significance have been studied intensively within the last 3 decades. This has been appreciated recently by the ASTM with two special conferences.[5,6)] The intrinsic resistance of metals against fatigue crack propagation is less systematically investigated. This is associated with the experimental difficulties to measure real intrinsic material data. So far, "intrinsic" data are always obtained from the total fatigue resistance of a material reduced by the extrinsic contribution obtained via crack closure measurements. Uncertainties and imprecisions during crack closure measurements therefore reflected themselves in the intrinsic crack growth curves.

The simulation of the intrinsic material resistance against cyclic plastic deformations at the crack tip has become feasible since the mid 80's due to an increasing computer power. The methods range from Finite Element simulations,[7–10)] mesoscale methods,[11–14)] and discrete dislocation modelling[15–21)] down to molecular dynamics simulations.[22)]

The aim of this paper is to summarize the recent modelling efforts to understand the near threshold behavior of cracks. The questions addressed within the paper are the following:

1. Why are different simulation techniques needed to understand the different aspects of fatigue crack growth?
2. What are the differences in the results of the discrete dislocation modelling and continuum plasticity and where are the similarities?
3. What is the intrinsic origin of the near threshold behavior of fatigue cracks?
4. How does microstructure influence the crack tip plasticity, and
5. is it possible to explain the minimum spacing of striations in the near threshold regime of fatigue cracks by dislocation mechanics.

2. The Length Scales Involved in Fatigue

To understand why we need different simulation techniques to model fatigue crack growth and why discrete dislocation models are appropriate for the description of the near threshold regime, we first consider an effective, *i.e.*, a crack closure corrected, crack growth curve. Such a curve is shown by the full circles in Fig. 1 (after Caton *et al.*[23)]) for aluminum alloy W319-T7 Al with a grain size of 23 μm. This crack growth curve is typical for a metallic material with an effective threshold of stress intensity range ($\Delta K_{\mathrm{th,eff}} \approx 0.8\,\mathrm{MPa}\sqrt{\mathrm{m}}$). It shows a sharp increase after the threshold, a midpart with a more moderate slope and a final increase at large stress intensity ranges which approach the quasi static fracture limit. The squares in Fig. 1 describe the cyclic plastic zone size, $\Delta\omega$, in dependence on ΔK based as a crude estimation, $\Delta\omega$ is about 3 orders of magnitude larger than the crack growth increment per loading cycle. The lower shaded stripe in Fig. 1 indicates a crack growth increment in the range of one Burgers vector

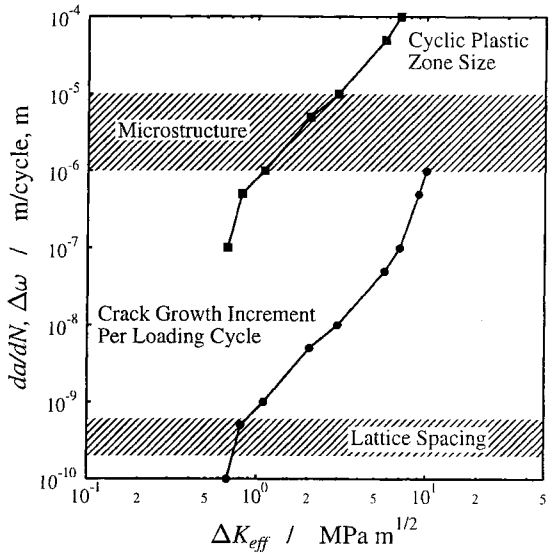

Fig. 1 An effective crack growth curve for an Aluminum alloy after.[23] Also shown is an estimation of the cyclic plastic zone size. The lattice spacing and the grain size are indicated by shaded stripes.

per loading cycle, the upper stripe indicates the grain size in this material. From this comparison we conclude the following:

- At moderate stress intensity ranges the cyclic plastic zone size, $\Delta\omega$, is smaller than or in the order of the grain size. $\Delta\omega$ becomes larger than microstructural features only for very large stress intensity factors.
- The crack growth increment per loading cycle shrinks to lattice dimensions in the lower part of the crack growth curve.

In essence, all length scales from atomistic to macroscopic are met along a crack growth curve which helps to understand why the variety of simulation methods already listed in the introduction is needed to describe all fatigue crack growth processes. While generally it is inconvenient to use lower hierarchical methods at higher physical levels, it is not only inaccurate but invalid to take higher hierarchical methods at lower physical levels. The physical length scale of the near threshold regime is the Burgers vector of the dislocations such that discrete dislocation models must be used to describe the near threshold plasticity. The Finite Element Method with continuum plasticity mechanics can be used to describe the macroscale plastic deformation in the upper Paris regime and above, mesoscale methods are appropriate for the lower Paris regime and the molecular dynamics simulations are useful to answer the question where plasticity comes from, *i.e.*, where and when dislocations are generated.

In the following the dislocation models proposed for the plastic deformation at cracks under near threshold conditions are briefly described and some differences between discrete and continuum plasticity are discussed. Then the influence of microstructure and of loading conditions (R-ratio) on the threshold and the near threshold plastic deformation is investigated.

3. Methodology

The plasticity in front of a mode II crack can be modelled as the motion of discrete dislocations on a slip plane which is coplanar to the crack. This is schematically depicted in Fig. 2.

The dislocations are generated at the crack tip when the local stress intensity factor at the crack tip exceeds a certain critical stress intensity factor for dislocation emission, k_e. Following Weertman[24] the shear stress acting on the emitted dislocation with the Burgers vector b at the position r ahead of the crack tip is given by:

$$\tau_{\text{dislocation}} = \frac{K_{II}}{\sqrt{2\pi r}} - \frac{\mu b}{4\pi r(1-\nu)} + \sum_{b'} \frac{\mu b'}{2\pi(1-\nu)} \sqrt{\frac{r'}{r}} \frac{1}{r-r'}, \quad (1)$$

where μ is the shear modulus and ν is Poisson's ratio. The sum in this equation is computed over all other dislocations at distances r' with the Burgers vector b'. The dislocation moves as long as the shear stress, $\tau_{\text{dislocation}}$, is larger than the local material resistance against slip, τ_{friction}. Since the emitted dislocation shields the crack, and reduces the local stress intensity factor, the next dislocation can only be generated after a certain increase of the applied load. Therefore the computer algorithm consists of:

1. seeking the equilibrium positions of the dislocations,
2. load increase (or decrease during unloading), and
3. dislocation emission.

The cyclic plastic deformation at the crack tip, $\Delta CTOD$, is obtained by counting the number ΔN of dislocations returning to the crack tip during unloading:

$$\Delta CTOD = \Delta N b. \quad (2)$$

This dislocation model, used by Pippan[17] for mode II and mode III cracks, was extended by Riemelmoser *et al.*[18] for a crack loaded in mode I where the plasticity takes place on shear planes inclined to the crack propagation plane. Wilkinson *et al.*[19] assumed again a mode II crack but with internal dislocation sources at some distance in front of the crack tip. The critical stress intensity factor for dislocation emission, k_e, is then replaced by a critical stress intensity factor to generate the dislocation at the source. The beginning of cyclic plastic deformation was found to be relatively insensitive to the friction stress and the dislocation source parameters, within a reasonable range. Doquet[20] used the same model as Pippan and incorporated the effect of friction at the crack flanks.

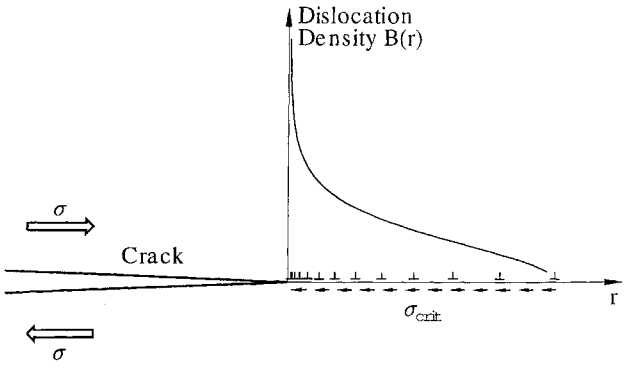

Fig. 2 A schematic dislocation arrangement in front of a mode II crack.

4. A Comparison of Discrete and Continuum Plasticity

In order to get a first impression of the similarities and the differences between discrete dislocation mechanics and continuum mechanics, the very simple system of a crack in a material with a friction stress which is uniform in space (homogeneous material) and time (non-hardening material) has been considered. This model material has been studied by several authors.[17–20] The general trend observed in these studies is shown in Fig. 3 (after[18]) where the $\Delta CTOD$ for a loading- and complete unloading cycle is depicted as a function of ΔK which has been normalized by the critical stress intensity factor for dislocation emission, k_e.

The result of the discrete dislocation model is drawn as a solid line in Fig. 3. The broken line in Fig. 3 is the prediction of a distributed dislocation simulation (after[25,26]) which is similar to the BCS model.[27] The distribution of dislocation model still describes plastic deformation as the consequence of dislocation motion but allows infinitesimally small Burgers vectors. Plasticity is therefore smeared-out along the shear plane such that it actually correspond to a continuum model. Figure 3 therefore allows to compare discrete plasticity with a continuum approach.

At stress intensity ranges greater than $3k_e$ the numbers of cyclically emitted and annihilated dislocations becomes large ($\Delta N > 100$) and the differences between discrete plasticity and continuum plasticity disappear. From the physical point of view both plasticity models are therefore equivalent in the limit of large plastic deformations. The difference lies in the numerical efficiency. At large ΔK-values, the calculation of a single point with the discrete dislocation model requires about 5 hours of CPU time on a modern workstation, while the entire $\Delta CTOD$ curve is computed within a minute or so when using the distributed dislocation technique. This clearly favors continuum mechancis for large plastic deformations. The reason for simulating plasticity as the motion of discrete dislocations is seen at small ΔK-values when the plastic deformation shrinks to some 10 Burgers vectors or below. For such a small number of cyclically moved dislocations, the plastic deformation is constrained by its discrete nature, a phenomenon which is naturally lost by the "smoothing procedure" of continuum approximations. This constraint leads to a sharp decrease of the plastic deformation at small ΔK-values where only 1 or 2 dislocations are moved. It culminates in the disappearance of any cyclic plastic deformation below a threshold value. Near the threshold the difference between the physical, *i.e.*, the discrete plastic deformation and the approximated one by the distributed dislocation technique is roughly 1 order of magnitude!

5. The Threshold of the Cyclic Plastic Deformation

The constraint on cracks due to the discreteness of plasticity impedes the plastic deformation at small stress intensity ranges and leads in the homogeneous material in Fig. 3 for loading-complete-unloading-cycles to a threshold at $\Delta K = 1.3k_e$. Naturally the question arises how different critical shear stresses, the presence of grain boundaries or dislocation obstacles and/or different mean loads influence the threshold value.

5.1 The influence of different critical shear stresses

The influence of different critical shear stresses on the threshold in homogeneous materials has been investigated in[17,19] (dislocation generation at the crack tip) and[28] (internal dislocation sources). These papers conclude in coincidence that the threshold of plastic deformation is always about 1.1 to $1.3k_e$. The threshold is therefore nearly independent of the friction stress and of the dislocation generation mechanism. For instance, Fig. 4 shows that $\Delta K_{th,intr}$ changes only by few per cent when the friction stress changes one order of magnitude (after[17]).

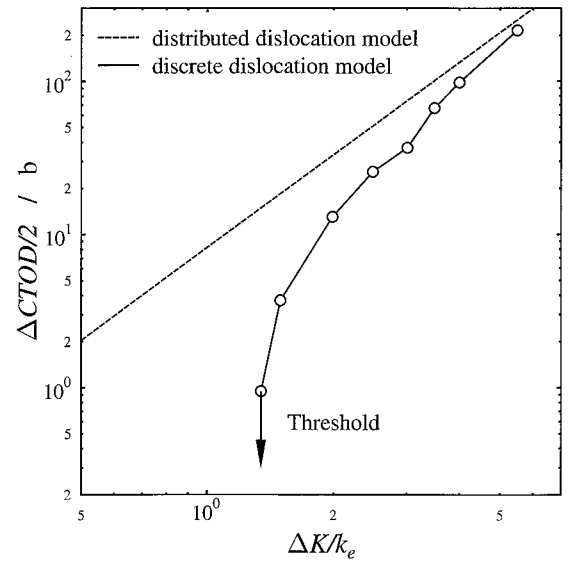

Fig. 3 The cyclic crack tip opening displacement as a function of ΔK for a stationary mode I crack at stress ratio, $R = 0$. Comparison between the discrete dislocation model and a distributed dislocation method, after.[18]

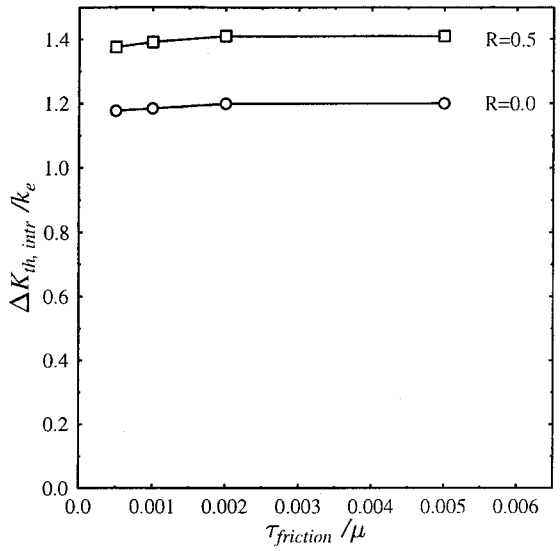

Fig. 4 Dependence of the threshold of cyclic plastic deformation on the friction stress in homogeneous materials, after.[17] The critical stress intensity range $k_e = 0.2G \cdot \sqrt{b}$, stress ratio $R = 0$ and 0.5 (R = minimum stress intensity factor, K_{min}/maximum stress intensity factor, K_{max}).

5.2 The influence of microstructure

The influence of the interaction of discrete dislocations and microstructure at near threshold conditions was considered in[29,30] (dislocation emission from the crack tip) and[28] (internal dislocation sources). The simulation techniques are the same as for homogeneous materials. A model grain structure in an isotropic elastic material is depicted in Fig. 5.

In the absence of an elastic mismatch or elastic anisotropy the effect of the grain boundaries (more generally, the dislocation obstacles) is to locally increase the resistance of the material against dislocation motion. Dislocations can overcome the grain boundary when the following dislocations increase the force on the leading dislocation until this force equals the grain boundary resistance.

The influence of the distance L between the crack tip and the single, penetrable dislocation obstacle on the threshold is displayed in Fig. 6 (after[30]). When the distance between the crack tip and the obstacle becomes larger than the cyclic plastic zone size, the threshold is independent of the obstacle strength and is the same as in the homogeneous material ($\Delta K_{\text{th}} = 1.1 k_e$). The predicted threshold value deviates from the homogeneous case for smaller L. The difference becomes larger than $k_e/2$ for very strong obstacles and at small distances between the crack tip and the obstacle (for $L < 1000$ Burgers vectors).

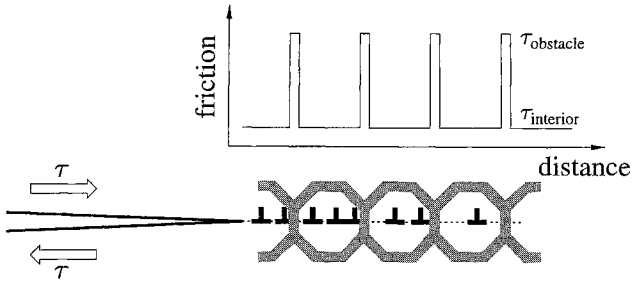

Fig. 5 A 2D model to simulate the influence of grain boundaries on near threshold crack propagation.

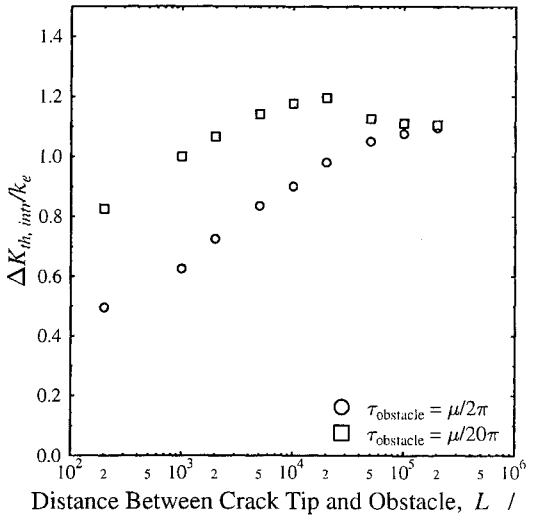

Fig. 6 Influence of dislocation obstacles on the threshold of plastic deformation, after.[30] The results have been obtained for the case that the first dislocation overcomes the obstacle. At lower maximum stress intensity factors-*i.e.*, at lower stress ratios-$\Delta K_{\text{th,intr}}$ is larger than the plotted values. At larger maximum stress intensity factors $\Delta K_{\text{th,intr}}$ is approximately constant, hence, the indicated values can be considered as lower limit values.

Strong obstacles can only be overcome by the help of a dislocation pile up. The space to build up such a pile up is limited, at small distances between the crack tip and the obstacle. The equilibrium distance of the crack tip and the nearest dislocation can become very small which causes the reduction of threshold for cyclic plastic deformation at such small L. The effect is more pronounced for the stronger obstacles and would further increase for inpenetrable obstacles ($\tau_{\text{obstacle}} \to \infty$).[30] The largest reasonable obstacle stress is the theoretical shear stress. This case is displayed with the circles in Fig. 6. For weaker obstacles the effect of the obstacles clearly depends on the obstacle strengths and distances. For the extrapolation of the results of this study to realistic microstructures one has to consider that the 2D model in Fig. 5 has all the grain boundaries oriented parallel to the crack front and perpendicular to the crack propagation direction. In the physical reality grain boundaries usually form a more irregular net with varying distances and angles between the crack front and the grain boundaries. Such 3D arrangements are probably best projected onto the 2D simulations by taking the mean distance of the dislocation obstacles as the characteristic length scale, L. A distance between the obstacle and the crack tip of about 1000 Burgers vectors (=300 nm) is a very small value. The obstacle strength is usually well below the theoretical shear strength of the material ($\mu/2\pi$) such that, for these physically relevant cases, the effect of obstacles should be reasonably small. The deviation from the threshold in obstacle free materials is less than 30%.

One of the questions which often arises in connection with discrete dislocation simulation is whether the experimentally well documented dependence of fatigue thresholds on grain size can be explained by such dislocation models (materials with smaller grains tend to have lower thresholds). This does not seem to be the case and the grain size dependence, therefore does not seem to be an intrinsic effect. This conclusion is reached mainly because of the following discrepancy between experiment and simulations:

- Usual grain sizes range from 5 µm up to 200 µm. The increase of the measured threshold due to that change of the grain size can be as large as 5 to 7 MPa$\sqrt{\text{m}}$ (typical for steels).
- The effect in the simulations becomes if at all pronounced only for distances (grain sizes) smaller than 300 nm. The predicted decrease of the threshold is about $k_e/3$ and spoken in absolute units this is only about 0.02–0.7 MPa$\sqrt{\text{m}}$ depending on the material.

The dependence of absolute thresholds on grain size is, therefore, to a major extent an extrinsic effect and is due to the contact of the rough fracture surfaces. The roughness induced closure is more pronounced in coarse grained materials which explains their higher thresholds.

5.3 The influence of the stress ratio

The experimentally determined threshold of stress intensity range for crack propagation, ΔK_{th}, under mode I loading is significantly influenced by the maximum stress intensity factor or the stress ratio $R = K_{\min}/K_{\max}$, which is the parameter used to describe the mean load effects in fa-

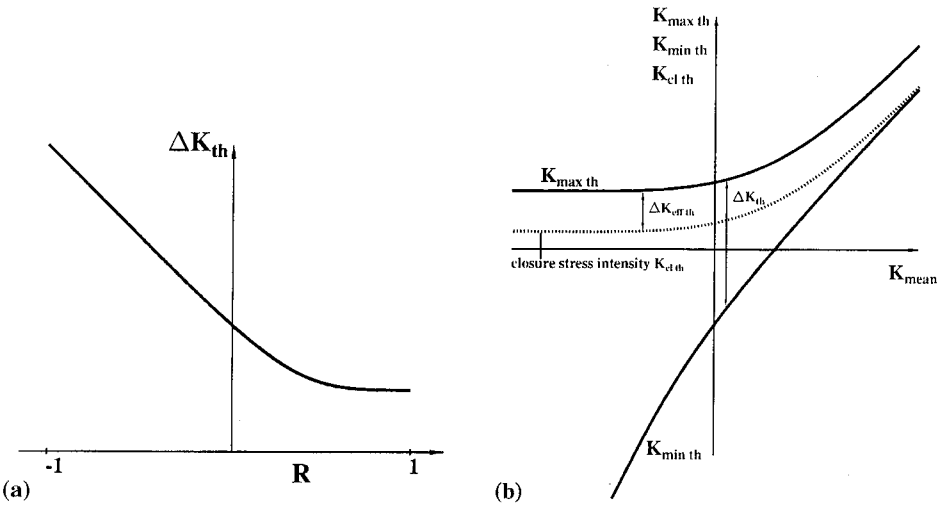

Fig. 7 Schematic representation of the R-ratio dependence of threshold for fatigue crack propagation under mode I loading. ΔK_{th} as a function of $R = K_{min}/K_{max}$ (a) and ΔK_{th} as a function of $K_{mean} = (K_{max} + K_{min})/2$ (b).

tigue. Figure 7 shows schematically the variation of ΔK_{th} as a function of R and the mean stress intensity factor, $K_{mean} = (K_{max} + K_{min})/2$. At negative R ratios ΔK_{th} increases continuously with decreasing R, at positive R ΔK_{th} decreases until at R ratios of 0.7 it reaches an approximately constant value.

Figure 8 shows schematically the threshold for cyclic plastic deformation as a function of the mean stress intensity factor, obtained from the discrete dislocation model. A consideration of the results for K_{mean} larger than 0 or, in terms of R for R ratios between -1 and 1, suggests that the R dependence of the threshold is induced by the intrinsic plastic deformation behavior under cyclic loading. At larger R ratios the distance between the nearest dislocation and the crack tip which is called the dislocation free zone decreases. This induces a reduction of the threshold of cyclic plastic deformation until it reaches an approximately constant value of $1.2k_e$. At stress ratios smaller than -1, dislocations with an opposite sign are generated during the "negative" phase of the load cycle, so that the dislocation free zone decreases again and $\Delta K_{th,intr}$ decreases in the same way as at $R > -1$.

The threshold for cyclic plastic deformation for stress ratios $R > 0$ is usually about $1.2k_e$. In order to understand that this threshold is larger at negative stress ratios a mode II crack at a stress ratio $R = -1$ is considered. In this case the mean value of the load is zero. At ΔK of $1.2k_e$ the maximum stress intensity factor is $K_{max} = +0.6k_e$ and $K_{min} = -0.6k_e$. Since neither K_{max} nor $|K_{min}|$ exceed the critical stress intensity factor for dislocation generation, k_e, no dislocations are generated and no plastic deformation occurs. The first dislocation is generated if $K_{max} = k_e$, it will return to the crack tip or a dislocation with an opposite sign of the Burgers vector will be generated at $K_{min} = -k_e$ (if no obstacles are located in the vicinity of the crack tip[30]). From these simple arguments one obtains a roof function of the threshold in dependence on the mean load as shown in Fig. 8 (A plot against the R-ratio would artificially introduce an asymmetric curve since the definition of R itself is inherently asymmetric).

The roof at mean stress intensity factors between $-0.5k_e < K_{mean} < 0.5k_e$ (corresponding to an R-ratio between 0 and $-\infty$) reflects that either the positive or the negative maximum stress intensity factor has to be larger than k_e in order to produce dislocations. These explanations are confirmed by the results in Fig. 9 obtained by discrete dislocation simulations.[31]

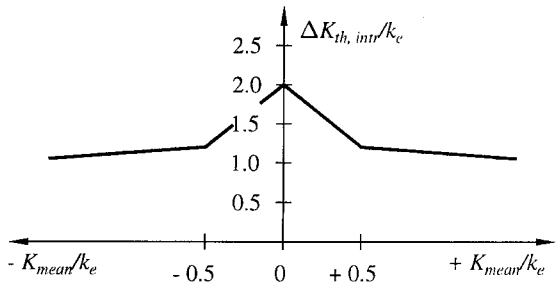

Fig. 8 Influence of the stress ratio on the threshold of cyclic plastic deformation at mode II or mode III crack.

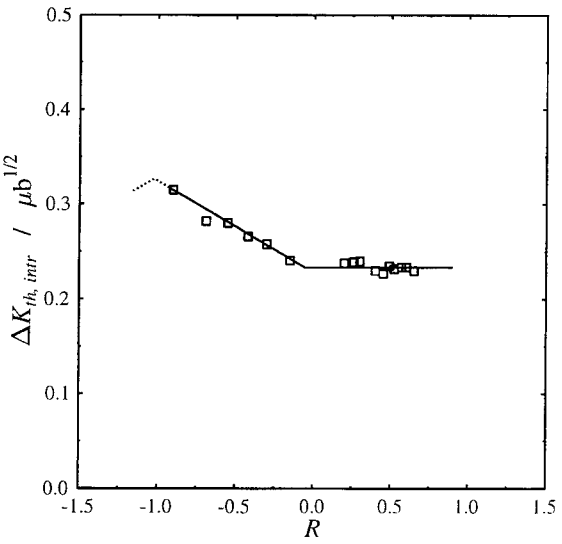

Fig. 9 The computed effect of the stress ratio on the threshold of cyclic plastic deformation, after.[31]

It must be emphasized that even at the maximum (at $R = -1$) the increase of ΔK_{th} is only about $0.1\mu\sqrt{b}$ (see Fig. 9),

and hence only between 0.2 and 0.7 MPa$\sqrt{m}$ for typical structural metals and alloys. The experimentally observed R-ratio effects vary from alloy to alloy and can be as large as 5 MPa$\sqrt{m}$ for R between -1 and 1. Furthermore, in the mode II and III simulation the effect is pronounced only for negative R-ratios. For a mode I loading we have to distinguish between an applied stress ratio, $R = K_{min}/K_{max}$, and a local stress ratio R^{local}. $R^{local} = K_{min}^{local}/K_{max}$ is the real acting stress ratio at the crack tip, where the local minimum stress intensity factor K_{min}^{local} is equal to the applied K_{min} if no crack contact occurs and K_{min}^{local} is equal to the crack closure stress intensity factor, K_{cl}, where a contact of the crack flanks takes place. Since K_{cl} is usually positive in the case of mode I loading, negative local stress ratios are unrealistic. Hence, the experimentally observed R-ratio effect must mainly be caused by crack closure (see also[32]).

5.4 Discussion of the proportionality of the threshold of cyclic plasticity and k_e

It appears to be somewhat paradoxical that the threshold of cyclic plasticity should be proportional to k_e–since the plasticity is obviously controlled by the motion of dislocations while k_e only reflects the nucleation event. The reason for this paradoxon is the development of a dislocation free zone (DFZ) ahead of the crack tip during loading and the stress distribution within the DFZ. Albeit existence of the threshold can be explained by the DFZ, it is not the case that the threshold directly correlates with the size of the DFZ. This can be seen by comparing two homogeneous materials with the same k_e but with different critical shear stresses. These materials have nearly the same threshold of the plastic deformation but the DFZ is much smaller in the material with the larger $\tau_{friction}$.

The DFZ displayed in Fig. 10 is defined as the elastic region between the last emitted dislocation and the crack tip. The elastic stress field within the DFZ is characterized by a local stress intensity factor, k_{local}. The value of k_{local} at maximum load is equal to or only somewhat smaller than k_e. If the dislocation configuration is frozen during unloading, the applied load has to be reduced by $\Delta K = 2k_e$ in order to change k_{local} from $+k_e$ to $-k_e$. At this point, dislocations with a negative sign of the Burgers vector would be generated at the crack tip and consequently, this would be the largest possible reduction of the stress intensity factor without causing cyclic plasticity. This load difference therefore corresponds to the upper limit of the threshold.

The lower threshold limit is obtained if we consider the backflow of the dislocations during unloading. The exact load reduction which is needed to cause the return of the dislocation can only be found in a full simulation. However, the load reduction must at least be large enough to turn the repelling elastic stresses within the DFZ at maximum load into attractive stresses, since the stresses at maximum load are given by $+k_e$. Hence, before the dislocations can return to the crack tip, the load reduction must at least bring this repelling singularity to zero. Hence, ΔK must be equal to k_e. Both the upper and the lower limit of the threshold are proportional to k_e and therefore control the threshold.

Only in the case of extreme strong obstacles located very near the crack tip the threshold of cyclic plasticity can be somewhat smaller than k_e (see Fig. 6). This is induced by the large repulsive forces of the dislocations in the dislocation pile up which is built up between the crack tip and the barrier. The repulsive forces cause a significant movement of the dislocations towards the crack tip which contributes to reduce the singularity at the crack tip.[30] It is interesting to note that these findings are quite contrary to the conventional feeling that a barrier such as a grain boundary which impedes the plastic deformation should rather increase the fatigue resistance. Here common sense is mislead because the intrinsic threshold is a phenomenon of the discreteness of plasticity with no macroscopic equivalent.

5.5 Comparison of predicted and measured intrinsic thresholds

Different authors show[33–35,46,47] that the intrinsic (≈effective) threshold is proportional to the Young's modulus and it is almost independent of the "plastic material properties" such as the microstructure and the macroscopic yield stress of the material. The constant of proportionality turns out to be approximately $1.6 \cdot 10^{-5}\sqrt{m}$. A similar result has been reported recently by Hertzberg.[34,35] He compared closure corrected stress intensity factor for steels, Aluminum alloys, Copper and Nickel alloys at a crack growth rate of 1 Burgers vector per cycle (*i.e.* almost at the threshold) and found that it is always about $\Delta K_{th,b} \approx E\sqrt{b}$.

Classical fatigue cracks are driven by the local cyclic plas-

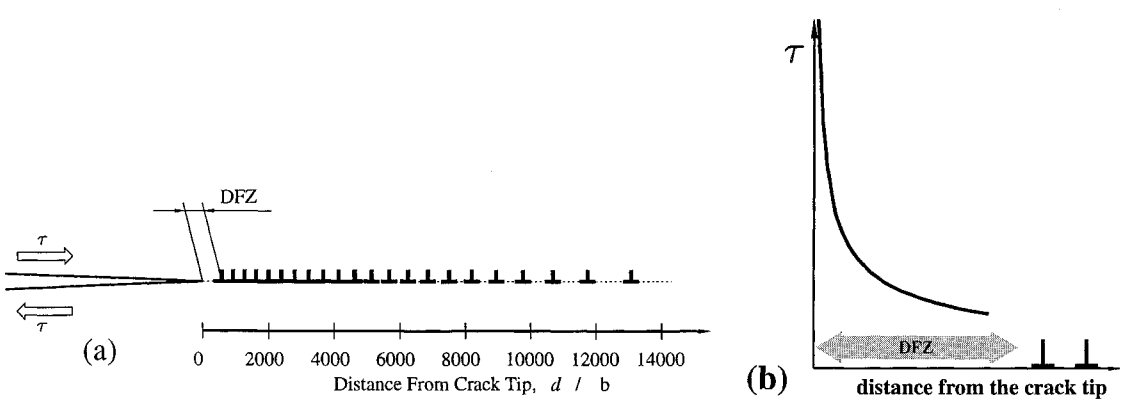

Fig. 10 The dislocation arrangement ahead of a mode II crack in plane strain and the definition of the dislocation free zone (DFZ) (a) and stress distribution within the DFZ (b). Material data: $\tau_{friction} = 0.002\mu$, $k_e = 0.2\mu\sqrt{b}$, $\nu = 0.3$. $K_{max} = 2.0k_e$.

ticity at the crack tip (one should not confuse this with subcritical or diffusive crack propagation). Such cracks cannot grow without a cyclic dislocation generation and annihilation and the lower limit of their intrinsic threshold necessarily identifies with the threshold of the plastic deformation obtained by the discrete dislocation model. The lower limit of the intrinsic threshold therefore is given by $1.3k_e$. The Rice-Thomson model[36] for dislocation generation at crack tips leads to an estimate of k_e and, hence, of the intrinsic threshold equal to:

$$\Delta K_{\text{th,intrinsic}} = f(\Theta)\mu\sqrt{b}. \tag{3}$$

Qualitatively, this result agrees with Hertzberg's observation $\Delta K_{\text{th}} \propto E\sqrt{b}$. Absolute values are compared for 3 materials in Table 1 (the dislocation model results are after Ref. 37), where dislocation generation is assumed at the crack tip). As can be seen, in spite of the use of the upper limit of k_e the measured thresholds still are up to a factor of 2 larger than predicted by the dislocation model. Similar trends using internal dislocation sources have been found in.[19] One reason for this systematic deviation between predicted and measured thresholds could be that the measured thresholds are in spite of large R-values still not completely closure free such that they are somewhat larger than the intrinsic thresholds.[46,47] Another possibility might be that real intrinsic thresholds are indeed larger than predicted by the discrete dislocation models. For instance, a protective oxide layer at the crack tip could increase the resistance against dislocation generation (k_e increase) and so contribute to the intrinsic threshold of the materials or the dislocation generation criterion is somewhat too simple.

5.6 Influence of the 3D microstructure on the near threshold behavior

Fully 3D dislocation simulations have been established by Kubin[38] for an infinite, uncracked, and homogeneous body and a few studies also consider crack-dislocation interactions in 3D (Devincre and Roberts,[39] Hartmaier and Gumbsch[48]). Because of the high numerical costs it is at the moment not possible to include also the effect of microstructure in these models which would be desireable to get reliable predictions of real fatigue crack behavior.

For the low temperature ductility of semi-brittle materials (*e.g.*, tungsten, molybdenum, Fe, *etc.*) and the ductile to brittle transition 3D effects of dislocation interaction seems to play an important role.[48] This raises the question why the 2D-dislocation model should predict the fatigue crack propagation behavior in the near threshold regime. There is a general difference between cleavage fracture or semi-brittle fracture (cleavage fracture where a certain amount at plastic deformation at the crack tip is involved) and fatigue crack propagation. The intrinsic mechanism of cleavage fracture is a breaking of individual atomic bonds at the crack tip along a certain plane or a coalescence of micro- or nanocracks nucleated ahead of the crack. The plastic deformation the movement of dislocations is in this case an extrinsic mechanism which changes the stress field of the crack tip. In contrast, the intrinsic fatigue crack propagation mechanism in ductile metals is the cyclic plastic deformation of the crack tip the blunting and resharpening of the tip. Therefore, dislocation movement and crack propagation are strongly coupled. At low propagation rates, the fatigue crack grows either along a slip plane or the crack front is formed by the intersection of two slip planes. This induces the formation of facets on the fracture surfaces. The size of the facets is in the order of microns and is much larger than the characteristic distance of dislocation motion (which is equal to the DFZ) near the threshold. Therefore, the propagation of real fatigue crack should be describable in a first approximation by a sum of 2D problems on different fracture facets.

Table 1 Comparison of measured and predicted effective threshold stress intensity ranges.

Alloy system	Measured effective threshold $\Delta K_{\text{th,eff}}$ in MPa$\sqrt{\text{m}}$	Hertzberg's estimate $E\sqrt{b}$ in MPa$\sqrt{\text{m}}$	Threshold of dislocation model $\Delta K_{\text{th,intr}}$ in MPa$\sqrt{\text{m}}$
Fe	3.0 ± 0.6	3.3	2.6
Al	1.4 ± 0.5	1.2	0.6
Cu	2.2 ± 0.7	1.9	0.9

Unfortunately, the understanding of 3D effects is incomplete from the experimental point of view, too. Yet the best and most promising model is due to Davidson.[41] He argues that at the crack front there are in a statistical average always grains with large Schmid factors and other less favorably oriented grains. If such a crack is loaded only somewhat above the threshold dislocations are produced and the crack grows only in the few favorable grains. The crack remains behind in the other grains. As a consequence an irregular crack front develops. This is accompanied by a decrease of the local stress intensity factor in the leading grains and an increase in the less favorable grains. Due to this load redistribution the crack starts to propagate in the backward grains and stops growing in the leading grains, in particular, when the crack front crosses the next grain boundary and enters into a grain with a smaller Schmid factor. Similar arguments should be applicable to lower level, the propagation along fracture facets.

Although this irregular crack propagation should hardly influence the threshold value itself, it has the important consequence that it causes crack growth rates below one Burgers vector per cycle. The macroscopic crack growth rate can be seen as an average over grains or facets where the crack does and does not propagate. The smallest measured crack growth rates usually are at about 1/10 to 1/100 Burgers vector per cycle. With a minimal crack growth rate of one Burgers vector per cycle in any particular grain or facet it requires the reasonable number of 10 to 100 grains or facets along the crack front with different orientations.

6. The Crack Tip Deformation above the Threshold

In what follows we return to the discussion at the beginning of the paper–*the length scales involved in fatigue*–but now from the theoretical point of view by considering the influence of the friction stress and of grain boundaries or lamellar structures on the cyclic plastic deformation at stress intensity ranges above the threshold.

6.1 The influence of the friction stress

The influence of different critical shear stresses on the plas-

tic deformation at a mode II crack is discussed in[28] (internal dislocation sources) and in[29] (dislocation emission from the crack tip). For the dislocation emission from the crack tip and for friction stresses of $\tau_{\text{friction}} = 0.001\,\mu$ and of $\tau_{\text{friction}} = 0.002\,\mu$ the results of a dislocation simulation are displayed in Fig. 11.

The curves in Fig. 11 display the same general behavior which has been indicated in Fig. 3 and which is also seen in many other "crack growth curves" of homogeneous materials published in the literature. At large stress intensity ranges the curves approach the continuum approximations (broken lines) which for the mode II crack of Fig. 11 can be computed by the BCS model[27]

$$\Delta CTOD = \frac{\Delta K_{\text{II}}^2(1-\nu)}{4\mu\tau_{\text{friction}}} \tag{4}$$

At small stress intensity ranges the continuum mechanics solution is too "soft" since it does not account for the constraint of plasticity due to its discrete nature. In Fig. 11 the continuum mechanical approximations is undoubtedly valid for cyclic plastic deformations larger than about 100 Burgers vectors per cycle. The range of the transition regime where this dislocation plasticity is important, becomes somewhat smaller for larger friction stress. For diffuse friction stresses on the order of $0.01\,\mu \approx 800$ MPa and above we have observed that the transition regime more or less disappears (*i.e.* continuum approximations are quite accurate nearly down to the threshold). Such large friction stresses, however, are unrealistic for most materials, with the exception of materials with a very fine microstructure like pearlitic steels with an interlamellar spacing below 1 μm (Sorbit). In such materials the combined effect of closely spaced dislocation obstacles can be regarded as equivalent to a very high diffuse friction stress. In other materials with a characteristic microstructural length scale (grain size, interlamellar spacing) larger than about 5 to 10 μm the dislocation obstacles act as discrete entities with a small diffuse friction stress in the interior of the grain and a large barrier stress at the dislocation obstacle. Such materials are discussed subsequently.

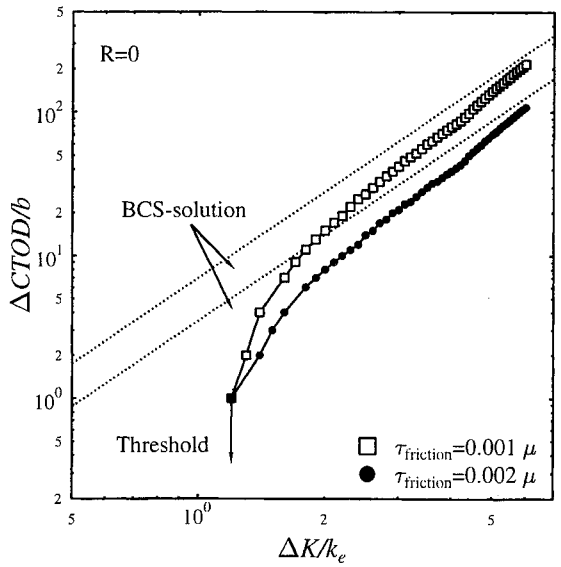

Fig. 11 The crack tip opening displacement as a function of ΔK. Comparison of two different critical shear stresses. $k_e = 0.2\mu\sqrt{b}$.

It is worth to point out that the predicted threshold for the two materials with a different friction stress displayed in Fig. 11 is the same and is therefore independent of the chosen friction stress. This result is contrary to what one would expect from purely continuum mechanical considerations. Even if an artificial "threshold criterion" is introduced into the continuum approach by truncating the continuum solution at a plastic deformation of one Burgers vector per cycle, the continuum solution would predict a larger threshold in the harder material. In the particular case of Fig. 11 it would be a factor of $\sqrt{2}$. Among other reasons discussed in this paper the failure of the continuum mechanic picture in reproducing the discrete dislocation results is why we conclude that continuum plasticity is not only an inaccurate but also an invalid method near the threshold.

6.2 Influence of grain boundaries

In this section a periodical arrangement of grain boundaries ahead of a mode II crack, schematically shown in Fig. 6 is considered. For three different distances, L, between the crack tip and the first grain boundary the computed $\Delta CTOD$ as a function of ΔK is depicted in Fig. 12.

A fine grained material with a grain size $d_{\text{grain}} = 3000b$ (Fig. 12A) and a coarse grained material with $d_{\text{grain}} = 10.000b$ (Fig. 12B) are studied. The labelling "fine grained" and "coarse grained" is meant in comparison with the size of the DFZ, which in the latter case is much smaller than the grain size and comparable in the former case. It is instructive to consider first the stress intensity range above $\Delta K = 5k_e$. In this regime the plastic deformation is insensitive to the actual location of the crack tip with respect to the grain boundaries, the curves for the 3 simulations in both figures collapse. The cyclic plastic deformation can be calculated by the BCS model with the assumption of a homogeneous macroscopic yield stress (broken lines). This loading regime is therefore called the macro mechanics regime of fatigue. Following the Hall-Petch model (see, *e.g.*,[42]), the macroscopic yield stress increases for smaller grains, and consequently a finer grained material gives a smaller $\Delta CTOD$ for a given ΔK than the coarse grained material. Within the BCS model this corresponds to macro stresses of $\tau_{\text{macro,fine}} = 250$ MPa and $\tau_{\text{macro,coarse}} = 190$ MPa.

At intermediate stress intensity ranges the plastic deformation is significantly influenced by the microstructure while the various curves approach each other again near the threshold.

The same trends but from a different perspective are seen in Fig. 13, which shows the $\Delta CTOD$-curves in the fine grained material as a function of the distance between the crack tip and the next grain boundary. The results are plotted for constant stress intensity ranges ($\Delta K/k_e = 1.5$, 2.5 and 4.5) which correspond to different mechanical crack growth regimes. Obviously, the plastic deformation is almost independent from the distance between the crack tip and the next grain boundary for the macro mechanics regime. This is different in the micromechanical regimes at intermediate stress intensity ranges. $\Delta CTOD$ becomes smaller when the crack tip approaches the grain boundary, where a grain boundary acts as a barrier for the plastic deformation. Such behavior has been observed also by analyses based on distributed dis-

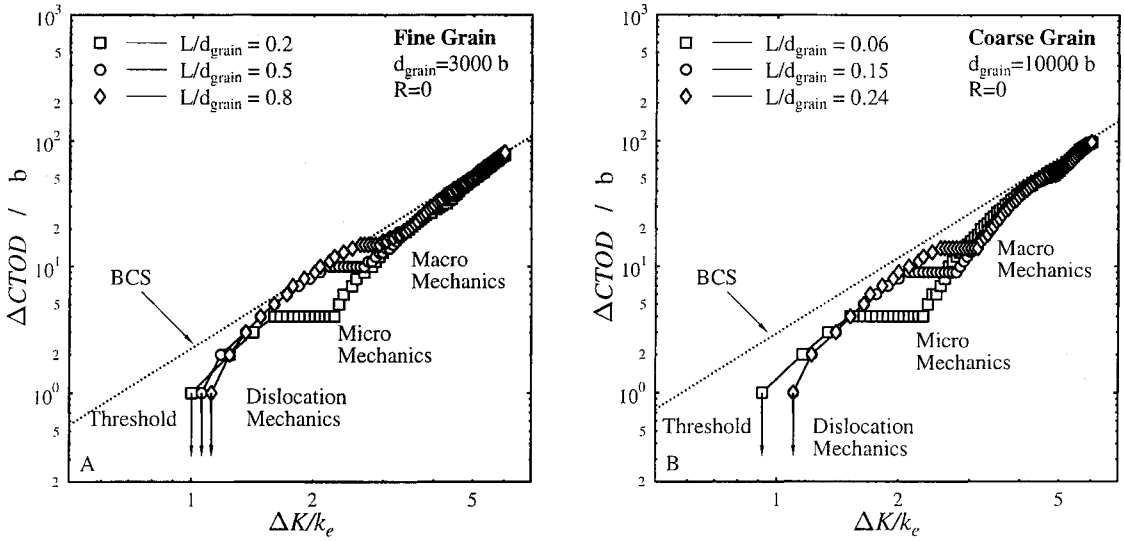

Fig. 12 The cyclic crack tip opening displacement at a mode II crack as a function of ΔK for 3 different distances to the first grain boundary (in both figures the distances between the crack tip and the nearest grain boundary are equal). Material data: $\tau_{\text{friction}} = 0.002\mu$, $\tau_{\text{barrier}} = 5\tau_{\text{friction}}$, $k_e = 0.2\mu\sqrt{b}$, $\nu = 0.3$. $R = 0$.

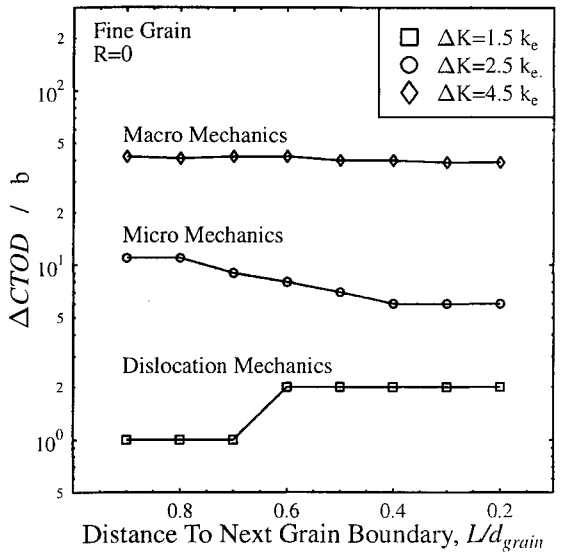

Fig. 13 The $\Delta CTOD$ in dependence on the distance between the crack tip and the nearest grain boundary for 3 different ΔK levels. Material data: $d_{\text{grain}} = 3000b$, $\tau_{\text{friction}} = 0.002\mu$, $\tau_{\text{barrier}} = 5\tau_{\text{friction}}$, $k_e = 0.2\mu\sqrt{b}$, $\nu = 0.3$, $R = 0$.

locations.[11–13] In this micromechanical regime a continuum analysis is still reasonable. However, the local variation of the yield resistance has to be taken into account explicitely.

Finally, close to the threshold of stress intensity range completely different relationships are seen. In our example the $\Delta CTOD$ even increases for smaller distances between the crack tip and the next grain boundary. This behavior is caused by discrete plasticity and therefore cannot be explained by continuum mechanical theory.

It is interesting to note that a comparison of Fig. 12 and Fig. 13 shows that at large stress intensity ranges, in the macro mechanics regime, the grain size turns out to be decisive for the cyclic plastic deformation at the crack tip but the location of the crack tip is unimportant. At small stress intensity ranges the opposite is true. Here the cyclic plastic deformations are controlled by the distance between the crack tip and the *next* grain boundary.

6.3 The influence of periodical layers with different plastic properties

Multilayer materials as sketched in Fig. 14 composed of two materials with the same isotropic elastic properties $E = 208$ GPa and $\nu = 0.3$ but a different critical resistance against plastic flow have been investigated by.[14] The α lamellae are softer and the β lamellae are harder $\tau_{\alpha,\text{friction}} = 80$ MPa and 240 MPa, respectively, and have a width of $W = 1.5\,\mu$m. Two simulations have been performed with a different location of the crack tip within the microstructure. The calculated $\Delta CTOD$ curves are depicted in Fig. 15 (the lower curves) for a location of the crack tip at the beginning of the softer α phase (circles) and at the beginning of the plastically harder β lamellae (squares).

The cyclic plastic zone size $\Delta\omega$ (upper curves), that is the size of the region of reverse plastic deformation during unloading, is seen to be 2 or 3 orders of magnitude larger than the $\Delta CTOD$ over the entire loading range. This is similarly predicted by continuum mechanics. The lattice spacing and the microstructural length scale are indicated by shaded stripes to show the good qualitative picture provided by discrete dislocation models (seen also in Fig. 1). From a qualitative point of view the behavior of the multilayer material is similar to materials with grains. At large stress intensity ranges the results are independent from the actual location of the crack tip. The broken asymptotic line was derived by the BCS solution with the assumption of a macroscopically averaged yield stress of the multilayer compound which in the particular case of Fig. 15 is $\tau_{\text{macroscale}} = \frac{\tau_{\alpha,\text{friction}}+\tau_{\beta,\text{friction}}}{2} =$ 160 MPa. A comparison with the cyclic plastic zone size shows that macroscale mechanics (with the assumption of a macroscale yield stress) becomes valid once $\Delta\omega$ exceeds about 5 times the microstructural length scale L. We have observed that, a similar relation holds also in materials with grains.

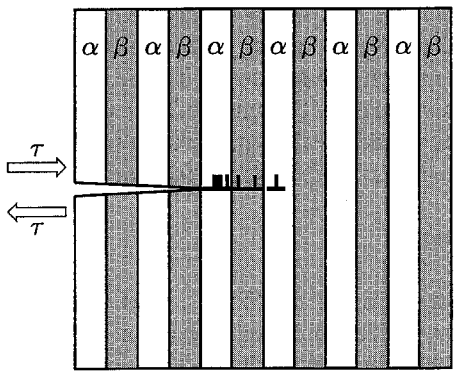

Fig. 14 A crack in a multilayer material subjected to a mode II loading.

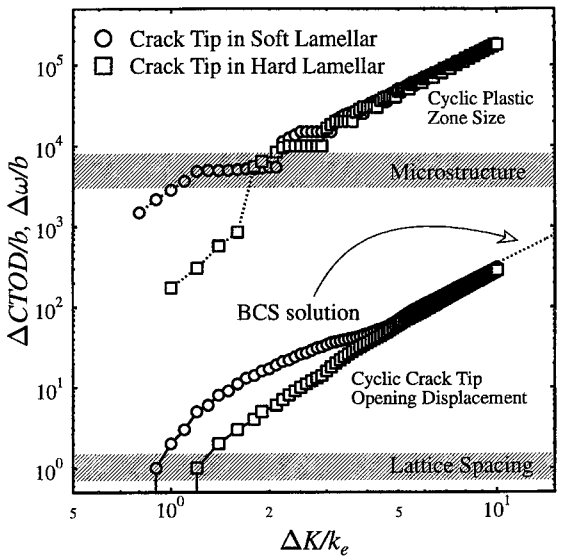

Fig. 15 The crack tip deformation and the cyclic plastic zone size in a multilayer material depending on the location of the crack tip.

At intermediate stress intensity ranges in Fig. 15, where the cyclic plastic zone size is in the order of the microstructural length scale, the 2 computed $\Delta CTOD$ curves deviate markedly. The plastic deformation is larger when the crack tip lies within the softer material. This is the micro mechanics regime of fatigue. At small stress intensity ranges the discreteness of plasticity becomes important which leads to a threshold at a cyclic plastic deformation of 1 Burgers vectors per cycle.

7. Comparison with Effective Crack Growth Curves

To overcome the difficulty introduced by crack closure, some effective crack growth data (=total fatigue resistance minus crack closure effects) are considered in Fig. 16 for a Ti- and Al-alloy and for 2 different steels, after Mabru *et al.*[51]

The effective stress intensity factor has been normalized by Hertzberg's[49] K_b. It is apparent that the effective crack growth data of the considered metals coincidence very well using this normalisation. This indicates that crack propagation at small stress intensity ranges is governed by a universal law which is more or less independent of material specific details, such as grain size, lattice type, *etc.*

The solid curve in Fig. 16, which agrees with the exper-

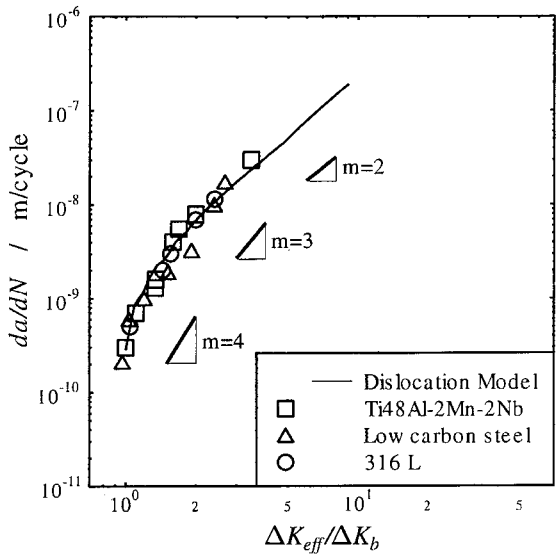

Fig. 16 Comparison of the prediction of the dislocation model with effective crack growth data.

imental data, is the predicted curve of the discrete dislocation model. For the calculation of this curve the $\Delta CTOD$-curve for the homogeneous material with a friction stress of $\tau_{\text{friction}} = 0.001\,\mu$ has been used and the relation $da/dN = \Delta CTOD$ with a Burgers vector of $b = 2.8 \cdot 10^{-10}$ m has been assumed. The excellent agreement between the simulation and the experimental data is certainly somewhat fortuitous and also depends somewhat on the choice of the model parameters, however, it is more important to realize that the "universal relation" controlling crack propagation at small stress intensity ranges is the manifestation of the constraint due to the discreteness of plasticity.

It is worth to note that the calculated $\Delta CTOD$ vs. ΔK curves in Figs. 12 and 15 show considerable microstructural dependence and, therefore, seem to contradict the universal nature of the curve in Fig. 16. However, comparing these curves, one has to take into account that the distance between the next grain or phase boundary varies in a realistic microstructure from zero to the grain diameter along the crack front. Therefore, a comparison of experimental data to the curves in Fig. 12 or Fig. 15 is possible only for the average, which should be similar to the curve of the homogeneous material in Fig. 16.

8. Dislocation Arrangement at Mode I Cracks

So far the dislocation models have been used to study the plastic deformation at a static crack, which is quite similar for mode I, mode II and mode III cracks (compare Figs. 3–11). The situation is the same for a growing mode II or a mode III fatigue crack since it does not leave dislocations in the wake of the crack tip. This is different in the case of a mode I crack. The simulation of a growing mode I crack requires the investigation of the effect of the dislocations which are left behind a propagating crack.[37] Such dislocations are called wake dislocations. These wake dislocations are responsible for the plasticity induced crack closure, which is extensively discussed in.[50] However, the plasticity induced crack closure is only

an effect of plasticity and not of the discreteness of plasticity. The discreteness manifests itself in the arrangement of the dislocations.

At small loading amplitudes the wake dislocations arrange in slip bands as shown in Fig. 17. The formation of these slip bands can be explained as follows. In the first loading sequence many dislocations are generated on the two inclined slip bands. During unloading few dislocations return to the crack tip where they annihilate. The remaining dislocations shield the crack tip and a much smaller number of dislocations is generated and annihilated during the second and many further loading cycles. By this blunting and "resharpening" process the crack propagates over a short distance and leaves the two slip bands behind the crack tip. As the crack tip moves away from the first two slip bands, their influence on the newly generated dislocations decreases. After a certain crack extension the interaction force between the pre-existing slip bands and the newly generated dislocations is small enough to let them pass the two pre-existing slip bands. A second pair of slip bands is formed. Similar processes in the further cycles lead to the dislocation arrangement schematically depicted in Fig. 17.

The distance between the slip bands turns out to be about 1500 to 2000 Burgers vectors but the crack growth rate is only few Burgers vector per cycle. Smaller distances between the slip bands do not occur because the elastic interaction stresses are too large. In the simulations the critical distance between the slip bands does not depend on the crack growth increment per load cycle. Each slip band leaves a step in the fracture surface such that this model predicts lines at the fracture surface parallel to the crack front with a characteristic distance in the order of some tenths of a micron. In[37] it was noted that this distance agrees with the minimum striation spacings observed in metals (see[43] for experimental observations).

A symmetric dislocation arrangement as shown in Fig. 17 is likely to occur at intermediate stress intensity ranges. At small stress intensity ranges, it is more often observed that the crack tip plasticity in a real crack is asymmetric like in the models proposed by Neumann[44] and by Pelloux.[45] It is obvious that the dislocation arrangement at the asymmetric crack is also governed by the dislocation-dislocation interaction forces which also lead to the distance between two large slip bands of the order of some tenths of a micron. Following this argument, the striations observed at small stress intensity ranges are traces of slip bands on the fracture surface.

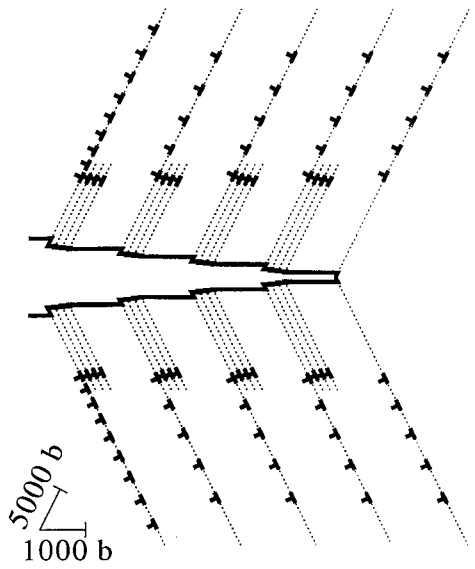

Fig. 17 The dislocation arrangement at a mode I crack, after.[37]

9. Summary

A consideration of the length scales involved in fatigue shows that the relevant length scale at threshold and near threshold conditions is the Burgers vector of lattice dislocations. Therefore the simulation models used to describe processes leading to the threshold of fatigue must contain the length of the Burgers vector to provide physically reasonable results. The appropriate simulation tools are discrete dislocation models which have been proposed within the past 20 years by several authors. The modelling efforts are summarized in order to document the progress in the understanding of the behavior of metals under fatigue loading. It is shown that the physical reason for the intrinsic threshold is induced by the discreteness of plasticity. Discrete plasticity leads to a sharp decrease of the crack growth curve below a cyclic plastic deformation of about 100 Burgers vectors per cycle and to a threshold of the plastic deformation at 1 Burgers vector per cycle.

It was shown that the intrinsic threshold of the plastic deformation does not depend significantly on the diffuse friction stress in homogeneous materials and the microstructure in structural material. The stress ratio, R, influences the intrinsic threshold only at small R values which are usually not important in the case of mode I loading. Furthermore, possible 3D effects on the threshold are discussed, and the predicted threshold is compared with measured effective thresholds. It is also shown how the plastic deformation above the threshold is influenced by the discreteness of plasticity in combination with the influence of grain boundaries and multilayers.

The results are compared with measured effective crack growth data. Good agreement between model prediction and experiments is observed.

In conclusion, plasticity and cracks at small stress intensity ranges have a peculiar behavior that cannot be explained by continuum (micro or macro) plasticity theories. It is hardly possible to over-emphasize that definitions, conceptions and quantities which are established in plasto-mechanics have no meaning for near threshold processes.

REFERENCES

1) P. C. Paris and F. Erdogan: J. Basic Eng. **85** (1963) 528–534.
2) W. Elber: Engineering Fracture Mechanics **2** (1970) 37–45.
3) R. O. Ritchie and S. Suresh: Metall. Trans. **13A** (1982) 937–40.
4) J. R. Rice: *Fatigue Crack Propagation*, ASTM STP 415, (Am. Soc. Testing Mats. 1967) 247–311.
5) J. C. Newman and W. Elber: *Special Technical Publication 982*, (Philadelphia, American Society of Testing and Materials, 1988).
6) J. C. Newman and C. R. McClung: *Special Technical Publication 1273*, (Philadelphia, American Society of Testing and Materials, 1998).
7) J. C. Newman Jr. and H. Armen: AIAA Journal **13** (1975) 1017–23.
8) R. C. McClung and H. Sehitoglu: Engineering Fracture Mechanics **33** (1989) 237–272.
9) R. C. McClung and D. L. Davidson: Engineering Fracture Mechanics **39** (1991) 113–130.

10) J. C. Newman Jr. C. A. Bigelow and K. N. Shivakumar: Engineering Fracture Mechanics **46** (1993) 1–13.
11) K. Tanaka and T. Mura: Acta Metall. **32** (1984) 1731–1740.
12) K. S. Ravichandran and E. S. Dwarakadasa: Acta Metall. Mater. **39** (1991) 1343–1357.
13) Li Xu-Dong and L. Edwards: Engineering Fracture Mechanics **54** (1996) 35–48.
14) F. O. Riemelmoser and R. Pippan: *Proceedings of Fatigue Crack Growth Thresholds, Endurance Limits and Design*, ASTM STP 1372, (ed. J. C. Newman and R. S. Piascik), (2000) 252–265.
15) T. Yokobori, A. T. Yokobori Jr. and A. Kamei: Philos. Mag. **30** (1974) 367–378.
16) J. C. M. Li: Scr. Metall. **20** (1986) 1477–1482.
17) R. Pippan: Acta Metall. Mater. **39** (1991) 255–262.
18) F. O. Riemelmoser, R. Pippan and H. P. Stüwe: Int. J. Fract. **85** (1997) 157–168.
19) A. J. Wilkinson, S. G. Roberts and P. B. Hirsch: Acta Metall. Mater. **46** (1998) 379–390.
20) V. Doquet: Fatigue & Fracture of Engineering Materials & Structures **21** (1998) 661–672.
21) R. Pippan and F. O. Riemelmoser: Kovove Materialy-Metallic Materials **36** (1998) 183–192.
22) H. Inoue, Y. Akahosi and S. Harada: Mater. Sci. Res. Int. **1** (1995) 95–99.
23) M. J. Caton, J. W. Jones, J. M. Boileau and J. E. Allison: Metall. Mater. Trans. **30A** (1999) 3055–3068.
24) J. Weertman, I.-H. Lin and R. Thomson: Acta Metall. **31** (1983) 473–482.
25) F. O. Riemelmoser and R. Pippan: *Proceedings, ICES 98: Modeling and Simulation Based Engineering II*, eds. S. N. Atluri and P. E. O'Donoghue (1998) 1456–1461.
26) F. O. Riemelmoser and R. Pippan: *Proceedings, International Symposium on Plasticity and its current applications* (1999) 791–793.
27) B. A. Bilby, A. H. Cottrell and K. H. Swinden: Proc. Roy. Soc. London. **A272** (1963) 304.
28) A. J. Wilkinson and S. G. Roberts: *Proceedings of the 6th International Fatigue Congress, Fatigue 99'*, eds. X. R. Wu and Z. G. Wang (1999) p. 678.
29) F. O. Riemelmoser and R. Pippan: *Proceedings of the 6th International Fatigue Congress, Fatigue 99'*, eds. X. R. Wu and Z. G. Wang (1999) 387–392.
30) R. Pippan: Int. J. Fracture **58** (1992) 305–318.
31) A. J. Wilkinson and S. G. Roberts: Scr. Mater. **35** (1996) 1365–1371.
32) A. J. McEvily and R. O. Ritchie: Fatigue & Fracture of Engineering Materials & Structures, **21** (1998), 847–855.
33) P. K. Liaw, T. R. Leax and W. A. Logsdon: Acta Metall. **31** (1983) 1581–1587.
34) R. W. Hertzberg: Int. J. Fracture **64** (1993) R53–58.
35) R. W. Hertzberg: Mater., Sci. Eng. **A190** (1995) 25–32.
36) J. R. Rice and R. Thomson: Philos. Mag. **29** (1974) 73.
37) F. O. Riemelmoser, R. Pippan and H. P. Stüwe: Acta Material. **46** (1998) 1793–1799.
38) L. P. Kubin: Phys. Status Solidi **135** (1993) 433–443.
39) B. Devincre and S. G. Roberts: Acta Material. **44** (1996) p. 2891–2900.
40) A. Hartmaier and P. Gumbsch: Physica Status Solidi B-Basic Research **202** (1997) R1–2.
41) D. L. Davidson: Private communication.
42) F. R. N. Nabarro: *Theory of crystal dislocations*, eds. N. F. Mott, E. C. Bullard, D. H. Wilkinson (Oxford University Press, London, 1967).
43) D. L. Davidson and J. Lankford: International material reviews **37** (1992) p. 45.
44) P. Neumann: Acta Metall. **17** (1969) 1219–1225.
45) R. M. N. Pelloux: Engineering Fracture Mechanics **1** (1970) 697–704.
46) R. Pippan: Philos. Mag. **77** (1998) 861–873.
47) R. Pippan, F. O. Riemelmoser and C. Bichler: ASTM STP **1343** (1999) 41–57.
48) A. Hartmaier and P. Gumbsch: Mat. Res. Soc. Porc. **539** (1999) 233–244.
49) A normalization with Young's modulus, E, as preferred by other authors[15,19,21] is similar because $K_b \approx E\sqrt{b}$ is itself proportional to E.[22,23]
50) F. O. Riemelmoser and R. Pippan: Fatigue & Fracture of Eng. Mat. & Struct. **21** (1998) 1425–1433.
51) C. Mabru, D. Bertheau, S. Pautrot, J. Petit and G. Hanaff: Engineering Fracture Mechanics **64** (1999) 23–47.